

# Soil moisture dynamics modelling enabled by hydraulic redistribution in multi-layer root zone

Rohitashw Kumar<sup>1,\*</sup>, Mahesh Kumar Jat<sup>2</sup> and Vijay Shankar<sup>3</sup>

<sup>1</sup>Division of Agricultural Engineering, Sher-e-Kashmir University of Agricultural Science and Technology of Kashmir, Shalimar Campus, Srinagar 190 025, India

<sup>2</sup>Department of Civil Engineering, Malaviya National Institute of Technology, Jaipur 302 017, India

<sup>3</sup>Department of Civil Engineering, National Institute of Technology, Hamirpur 177 005, India

**Moisture uptake by plant roots from unsaturated soil is a key process for plant growth and transport of water in the soil–plant system. A soil water uptake model was developed and validated for non-uniform crop root zone in a sub-temperate, sub-humid agro-climate of Solan, Himachal Pradesh, India. Root water uptake function was incorporated in the governing soil moisture flow equation. A nonlinear root water uptake model developed earlier was selected as the base model to evaluate moisture extraction pattern in multilayer crop root zone and to evaluate its efficacy for the agro-climate of Solan. To validate the enhanced prediction efficiency of the model for a multilayer crop root zone, field experiments were conducted at the sub-temperate, sub-humid agro-climate of Solan under controlled condition on pea (*Pisum sativum*). Model predicted soil-moisture parameters, i.e. moisture depletion, moisture status at various depths and soil moisture profile in the root are satisfactory and in good agreement with experimental results. The model results indicate that the moisture uptake is more near the base of the root system (i.e. close to the ground surface) and near the root tips compared to the middle region of the root system. The results validated the utility of the root water uptake model across different agro-climates for non-uniform soils having different soil-moisture characteristics in different layers of the root zone. The model has demonstrated its applicability for accurate estimation of crop water requirement and helps in better irrigation scheduling and water management.**

**Keywords:** Crop root zone, evapotranspiration, irrigation, mathematical modelling, soil–water.

QUANTITATIVE study of water movement in the soil–root system is an important component in the modelling of root water uptake (RWU) by crops and provides key information for optimum irrigation scheduling and water resources management. The movement of water from soil to plant roots was first established experimentally by Kramer<sup>1</sup>, since then it has been studied for a wide variety

of plant species across a range of dry and wet climate<sup>2–5</sup>. The boundary between soil and root system of plants is a major hydrologic interface across which over 50% of evapotranspiration takes place<sup>6</sup>. Molz and Remson<sup>7</sup> classified such studies into two categories. The first category follows a microscopic approach that studies radial flow of water to a single root and has contributed significantly to the understanding of RWU process<sup>8–11</sup>. The second category follows a macroscopic approach, in which the entire root system is treated as a single unit to sum up the effects of all individual roots<sup>12–19</sup>. The macroscopic approach has significant advantages over the microscopic approach<sup>20–23</sup>.

The root system extracts different volumes of moisture from the root zone, which is a function of location (depth from ground), moisture content and time. The soil–plant conductivity in the root system is significantly larger than that of the surrounding soil<sup>24</sup>, resulting in conductivity rates that are substantially larger than the soil matrix<sup>25</sup>. The moisture transport is determined by the soil water potential gradients and results in the movement of moisture deeper in the soil column during the wet season<sup>26–29</sup>, and transport of moisture from deep to shallow layers during the dry season<sup>30,31</sup>. The roots spread laterally when a strong gradient in soil water potential is imposed across the breadth of a plant root system<sup>4,32</sup>.

Ojha and Rai<sup>33</sup> developed a nonlinear RWU model. This is a particular case of linear and constant rate extraction model for  $\beta = 0$  and  $\beta = 1$  respectively ( $\beta$  is the Ojha and Rai model nonlinearity coefficient). Shankar *et al.*<sup>23</sup> developed a methodology for the Ojha and Rai<sup>33</sup> moisture uptake model from measurable plant physiological parameters such as maximum daily transpiration, maximum root depth and time to attain the maximum transpiration. A non-dimensional parameter, termed specific transpiration, involving the plant physiological parameters was used in this empirical relationship. Soil moisture uptake by plant roots is a dynamic process influenced by the plant characteristics, atmospheric demand, soil moisture availability and its hydraulic properties. In the macroscopic approach the RWU model is represented by a volumetric sink term, which is added to the Richards equation<sup>34</sup>, that describes moisture movement in the unsaturated zone.

\*For correspondence. (e-mail: rohituhf@rediffmail.com)

The root water extraction models can be classified into constant, linear and nonlinear<sup>13,17,22,33,35-39</sup>.

The present study describes a root uptake model for a multilayered crop zone and its validation through field experiments for pea crop in a sub-temperate, sub-humid agro-climate of Solan, Himachal Pradesh, India. A nonlinear macroscopic RWU model was validated for multi-layered crop root zone to predict the water uptake by plants and the hydraulic regime of the soil profile for different boundary conditions.

**Materials and methods**

*Water flow equation*

The movement of soil moisture in saturated soils in the presence of water uptake by plant root is important for the prediction of extraction rate by the root biomass. Richards equation<sup>34</sup> describes the moisture flow in unsaturated soil. A volumetric sink term was added in the Richards equation to account for moisture uptake by the roots. For one-dimensional vertical flow in cropped soil, mixed form of the Richards equation with a sink term is given as<sup>40</sup>

$$\frac{\partial}{\partial z} \left[ K(h) \left( \frac{\partial h}{\partial z} + 1 \right) \right] + S(z, t) = \frac{\partial \theta}{\partial t}, \tag{1}$$

where  $h$  is the pressure head,  $\theta$  (a function of  $h$ ) the volumetric moisture content,  $K$  (a function of  $h$ ) the hydraulic conductivity,  $S(z, t)$  the water uptake by roots expressed as volume of water per unit volume of soil per unit time,  $t$  the time and  $z$  is the vertical distance measured positively upwards. Equation (1) is highly nonlinear, as  $K$  and  $\theta$  are nonlinear functions of the dependent variable  $h$ . To solve this parabolic partial differential equation, explicit expressions for soil constitutive relationship between the dependent variable  $h$  and the nonlinear terms  $K$  and  $\theta$  are required. Therefore, numerical approximations are necessary to solve the above equation. The mathematical expressions used for describing the relationships between  $\theta$ ,  $h$  and  $K$  of the soil are collectively referred to as the soil constitutive relationships. In the present study, Van Genuchten<sup>41</sup> relationships are adopted for  $K$ - $\theta$ - $h$  and  $K$ - $\theta$  relationships, because of wide applicability of their parametrics which are given as follows

$\theta$ - $h$  relationship

$$\Theta = \left[ \frac{1}{1 + |\alpha_v h|^{m_v}} \right]^m \quad \text{for } h < 0, \\ = 1 \quad \text{for } h \geq 0, \tag{2}$$

where  $\alpha_v$  and  $n_v$  are unsaturated soil parameters with  $m = 1 - (1/n_v)$  for ( $n_v > 1$ ) and  $\Theta$  is the effective saturation defined as

$$\Theta = \frac{\theta - \theta_R}{\theta_s - \theta_R}, \tag{3}$$

where  $\theta_s$  is the saturated moisture content and  $\theta_R$  the residual moisture content of the soil.

*K- $\theta$  relationship*

$$K = K_{\text{Sat}} \Theta^{1/2} [1 - (1 - \Theta^{1/m})]^2 \quad \text{for } h < 0, \\ = K_{\text{Sat}} \quad \text{for } h \geq 0, \tag{4}$$

where  $K_{\text{Sat}}$  is the saturated hydraulic conductivity of the soil.

*Ojha and Rai model (O-R)*

Ojha and Rai<sup>33</sup> proposed a nonlinear RWU model to distribute the entire moisture extraction in the root zone. For potential transpiration conditions, the potential rate of soil water extraction  $S_{\text{Max}}$  is given by the relation

$$S_{\text{Max}} = \alpha \left[ 1 - \left( \frac{z}{z_{Rj}} \right) \right]^\beta \quad 0 \leq z \leq z_{Rj}, \tag{5}$$

where  $\alpha$ ,  $\beta$  are the model parameters,  $z$  the depth below soil surface and  $z_{Rj}$  is root depth on the  $j$ th day. For  $z = z_{Rj}$ ,  $S_{\text{Max}}$  is zero according to eq. (5) and at  $z = 0$ ,  $S_{\text{Max}}$  attains a maximum value. Thus eq. (5) satisfies the desired extraction conditions, i.e. extraction is maximum at the top and zero at the bottom of the root.  $S_{\text{Max}}$  is obtained as

$$S_{\text{Max}} = \left[ \frac{T_j}{z_{Rj}} (\beta + 1) \left( 1 - \frac{z}{z_{Rj}} \right)^\beta \right] \quad 0 \leq z \leq z_{Rj}. \tag{6}$$

For  $\beta = 0$ , eq. (6) gets converted to constant rate extraction model of Feddes *et al.*<sup>13</sup>, and for  $\beta = 1$  to the linear extraction model of Prasad<sup>36</sup>.

*Boundary conditions*

For numerical solution of eq. (1), certain initial and boundary conditions must be specified for the solution domain to get a particular solution. For initial condition of the field experimental data, measured values of the pressure head in the soil depth have been used. Hence

$$\left. \begin{aligned} h &= h_M(z) \\ h &= h_{Fc}(z) \end{aligned} \right\} \quad 0 \leq z \leq L, t = 0. \tag{7}$$

Here,  $h_M$  is the measured pressure head value in the field,  $h_{Fc}$  is the suction head corresponding to the field capacity, and  $L$  is the length of solution domain. The processes that take place at the soil surface are considered as the upper boundary condition. These processes are evaporation (in case of bare soil), evapotranspiration (in case of cropped soil) and infiltration (due to rainfall or irrigation). The upper boundary condition is a prescribed flux-type boundary condition accounting for the soil evaporation ( $E_s$ ), taking place from the topsoil and a Dirichlet-type boundary condition, during irrigation/rainfall, i.e.

$$h = h_{ir} \quad z = L, \text{ during irrigation/rainfall, (8)}$$

$$-K(h) \left( \frac{\partial h}{\partial z} + 1 \right) = E_s \quad z = L, \text{ in absence of irrigation. (9)}$$

Here,  $h_{ir}$  is the pressure head corresponding to saturated moisture content ( $h = 0$ ) during irrigation or rainfall.  $E_s$  is obtained as the partitioned component of the crop evapotranspiration. The groundwater table is at a considerably greater depth compared to the crop root zone. Hence gravity drainage-type condition has been adopted as the lower boundary condition, i.e.

$$-K(h) \left( \frac{\partial h}{\partial z} + 1 \right) = -K(h) \quad \text{for } t \geq 0, z = 0. \quad (10)$$

### Simulation procedure of governing equation

The differential eq. (1) along with initial and boundary conditions given in eqs (7)–(10) have been solved by a mass conservative, fully implicit finite difference scheme proposed by Celia *et al.*<sup>40</sup>. The differential moisture flow equation (eq. (1)) is first discretized numerically in time and space using an implicit finite difference method coupled with the Picard iteration scheme. The soil constitutive relationships are used to simulate the soil hydraulic parameters at each time level. The prescribed moisture content or flux boundary condition that signifies applied irrigation, rainfall or evaporation at the top node and either a known soil water pressure head or water flux at the bottom node defining the lower boundary is assigned. For each iteration, a set of algebraic equations in tri-diagonal form is formulated and solved using the Thomas algorithm to obtain the soil pressure head at all nodes along the depth of the root zone<sup>42</sup>. The iterative process continues until a satisfactory degree of convergence (absolute change in pressure head between two successive iterations becomes less than a predefined small value) at all nodes is reached.

A software code in FORTRAN 90 is developed for solution of governing equation. The soil profile up to 1.2 m is fairly uniform in texture but has different hydraulic properties. The soil column is divided in four

layers (0–30, 30–60, 60–90 and 90–120 cm) based on hydraulic properties of the soil in crop root zone. In the developed software code, different boundary conditions for different layers have been incorporated. While formulating the numerical model, the notation for the soil properties for different layers, e.g. saturated hydraulic conductivity has been denoted as KSAT1, KSAT2, KSAT3 and KSAT4 in layers 1, 2, 3 and 4 respectively (other soil layer properties are also incorporated on similar lines). The boundary condition for bottom node, top node and the layers between them is also incorporated in the model. Interface between any two layers is implemented in model. There are only three interfaces, i.e. between layers 1 and 2, layers 2 and 3, as well as layers 3 and 4. At interface nodes, an average value of soil properties has been considered. The input data to the numerical model have been supplied accordingly. The model was run for different cases and results were obtained accordingly.

For quantitative evaluation of model performance, error statistics parameters, e.g. co-efficient of determination (COD), coefficient of variation (COV) and average relative error (ARE) are used<sup>43</sup>. COD is defined as<sup>44</sup>

$$\text{COD} = 1 - \frac{\sum_{i=1}^n (\theta_{Mi} - \theta_{Si})^2}{\sum_{i=1}^n (\theta_{Mi} - \theta_{Avg})^2}, \quad (11)$$

where  $\theta_{Mi}$  is the field-observed percentage moisture depletion,  $\theta_{Si}$  the model-computed percentage moisture depletion,  $\theta_{Avg}$  the average of field-observed percentage moisture depletion values and  $n$  is the number of observations. For a perfect fit, COD equals unity. In addition, a quantitative assessment procedure has been followed, which involves the use of error statistics<sup>43</sup>, COV and ARE given by the equations

$$\text{COV} = \frac{\left[ \sum_{i=1}^n \frac{(\theta_{Si} - \theta_{Mi})^2}{n} \right]^{0.5}}{|\theta_M|}, \quad (12)$$

$$\text{ARE} = \frac{\sum_{i=1}^n (\theta_{Si} - \theta_{Mi})}{n |\theta_M|} \quad (13)$$

where  $\theta_{Si}$  is the model-predicted percentage moisture depletion in  $i$ th layer,  $\theta_{Mi}$  the corresponding field observed value,  $\theta_M$  the average of the field-measured moisture depletion in root zone layers, and  $n$  is the number of layers, into which the root zone is divided. A value of COD close to the unity indicates a high degree of association between the observed and simulated values.

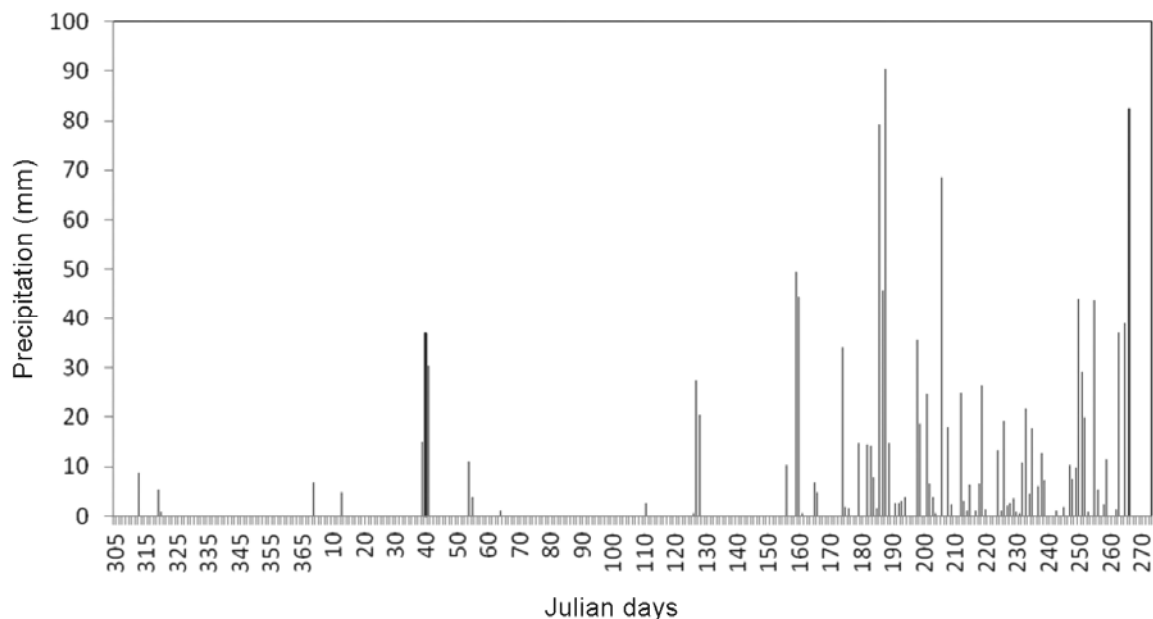


**Figure 1.** Daily precipitation from 1 November 2009 to 30 September 2010 at Solan, Himachal Pradesh.

COV quantifies the amount of random scatter of the simulated and measured values about 1 : 1 line<sup>45</sup> and ARE quantifies the extent to which model simulations overestimate (positive ARE) or underestimate (negative ARE) the values.

### Study area

Field experiments on pea crop were conducted during November 2009 to February 2010 at Dr Y.S. Parmar University of Horticulture and Forestry, Solan. The average rainfall in the area ranges from 1100 to 1300 mm with most of the rainfall occurring during monsoon season, i.e. June–September. Pan evaporation rate ranges from 1 to 12 mm/day. All the meteorological data required for the estimation of reference evapotranspiration have been obtained from the All Weather Station at the University. The rainfall pattern during field experiments is shown in Figure 1. The experiment includes the measurement of (i) crop evapotranspiration, (ii) plant parameters such as root depth, plant height and leaf area index (LAI) and (iii) soil parameters such as soil texture, bulk density, particle density, porosity, saturated hydraulic conductivity, soil moisture characteristics (SMC), field capacity and wilting point. The soil properties were measured as follows: soil texture analysis using sieve and hydrometer, bulk density using core sampler, particle density using pycnometer, saturated hydraulic conductivity using Guelph-type permeameter and pressure head using sensors. Plant parameters, i.e. LAI, crop height and root depth were measured using digital planimeter, measuring tape and trench profile respectively.

Drainage-type lysimeter (1.5 m deep with a surface area of 1 m<sup>2</sup>) was installed in an open field to avoid boundary effects and to simulate actual field conditions (Figure 2). The upper 1.3 m of the lysimeter was filled with a loam textured soil, maintaining hydraulic characteristics of soil in layers similar to original field conditions throughout the soil profile, characterized by an organic matter content of 1.1–1.2%. For measurement of soil suction head an advanced system of the soil moisture measurement sensors (Watermark, Irrrometer Company Inc., Riverside, CA), was installed. The sensors can measure soil pressure head in a range 0–199 centibars. In the experimental plot moisture measurement sensors were installed at a depth of 0.3, 0.6, 0.9 and 1.2 m. The watermark meter directly gives the soil pressure head value and is equipped with temperature adjustment setting. The measured suction heads have been converted into the corresponding moisture contents using field-calibrated constitutive relationships given by Van Genuchten<sup>41</sup>.

### Soil characteristics

Soil samples were obtained from 0.0 to 0.15, 0.15 to 0.3, 0.3 to 0.6, 0.6 to 0.9 and 0.9 to 1.20 m depths, from three locations, within the experimental site to determine soil characteristics. These samples were subjected to a detailed grain-size analysis using a set of standard sieves and a calibrated hydrometer<sup>46</sup>. Significant difference in soil moisture parameters was observed for different layers (Table 1).

The SMC express the functional relationship between the volumetric moisture content ( $\theta$ ) and the pressure head

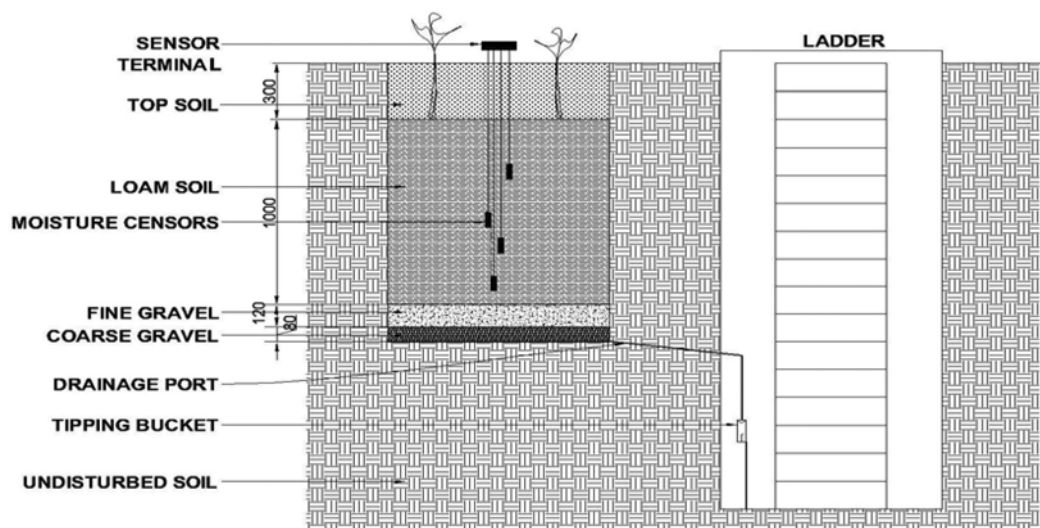


Figure 2. Lysimeter set-up.

Table 1. Texture and soil properties at different depths

Soil depth (cm)	Gravel (%)	Sand (%)	Silt (%)	Clay (%)	Particle density (g/cm <sup>3</sup> )	Saturated hydraulic conductivity (cm/h)	Field capacity (Fc) (cm <sup>3</sup> /cm <sup>3</sup> )	Permanent wilting point (cm <sup>3</sup> /cm <sup>3</sup> )	Available water (cm <sup>3</sup> /cm <sup>3</sup> )	Bulk density (g/cm <sup>3</sup> )
0–30	35.0	47.4	31.2	21.4	2.45	1.05	0.24	0.13	0.12	1.23
30–60	40.40	39.2	35.20	25.6	2.54	0.90	0.23	0.12	0.11	1.30
60–90	36.0	41.0	32.6	26.4	2.51	0.86	0.24	0.13	0.11	1.31
90–120	20.0	39.6	36.40	24.0	2.48	0.80	0.24	0.12	0.12	1.35

( $h$ ) in an unsaturated porous medium. The saturated moisture content  $\theta_s$  is assumed to be equal to the measured total soil porosity ( $0.50 \text{ cm}^3 \text{ cm}^{-3}$ ). In the absence of laboratory pressure plate apparatus, moisture content at such large matric potential cannot be determined, and hence a standard residual moisture content value equal to  $0.078 \text{ cm}^3 \text{ cm}^{-3}$  for loam soil has been adopted<sup>47</sup>. The *in situ* SMC are assumed to be described by the continuous and realistic Van Genuchten model, with values of unsaturated soil parameters  $\alpha_V$  and  $n_V$  as  $0.036 \text{ cm}^{-1}$  and  $1.56$  respectively. As soil texture in whole root zone is loam type, therefore the same value of  $\alpha_V$ ,  $n_V$  and  $\theta_R$  has been adopted. However, hydraulic conductivity, saturated moisture content ( $\theta_s$ ), permanent wilting point and field capacity were considered to be different for different layers.

### Crop parameters

Three major factors, LAI, plant height and root depth were recorded at discrete time intervals throughout the crop period during crop growth in the experimental plots. Due to differences in evapotranspiration during the various growth stages, the crop coefficient ( $K_C$ ) for a given crop has been used which varies over the growing period.

The growing period is divided into four distinct growth stages, viz. initial, crop development, mid-season and late season denoted by stages I–IV respectively. Growth stages have been considered on the basis of a study by Doorenbos and Pruitt<sup>48</sup>. Details of crops grown are shown in Table 2. The variation of LAI, crop height and root depth during the crop period is shown in Figure 3. Maximum root depth has been observed during the mid-season stage of crop as 57th days after sowing (DAS) for pea (0.65 m).

Crop evapotranspiration mainly consists of three parameters, soil evaporation, plant transpiration and interception. Partitioning equation based on LIA has been used in the present study to partition soil evaporation and plant transpiration<sup>49–51</sup>.

$$\frac{E_s}{ET_C} = \text{EXP}(-\delta * \text{LAI}), \quad (14)$$

where  $\delta$  is the dimensionless canopy extinction coefficient, whose value is  $0.48$  for pea<sup>52</sup>. Daily crop evapotranspiration and its components, i.e. transpiration and evaporation for pea are shown in Figure 4. The maximum value of transpiration was observed as  $1.66 \text{ mm/day}$  on 57th DAS for pea.

**Table 2.** Details of pea crop

Variety sown	Date of sowing	Date of harvesting	Crop period (days)	Growth stage (days)				Irrigation provided (day no.)	Spacing (cm)
				I	II	III	IV		
Arkal	24 November 2009 Julian day-328	3 March 2010 Julian day-62	100	20	25	30	25	19, 21, 39, 68 and 79	45 × 5

I, Initial; II, Development; III, Mid-season; IV, Late season.

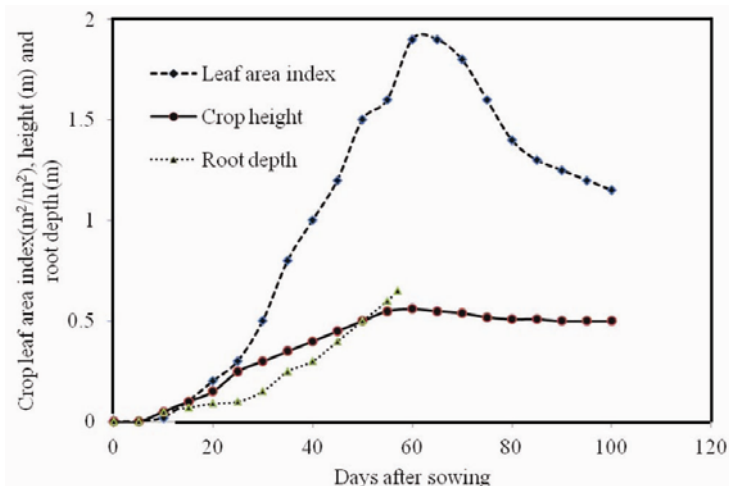


**Figure 3.** Variation in leaf area index, crop height and root depth of pea.

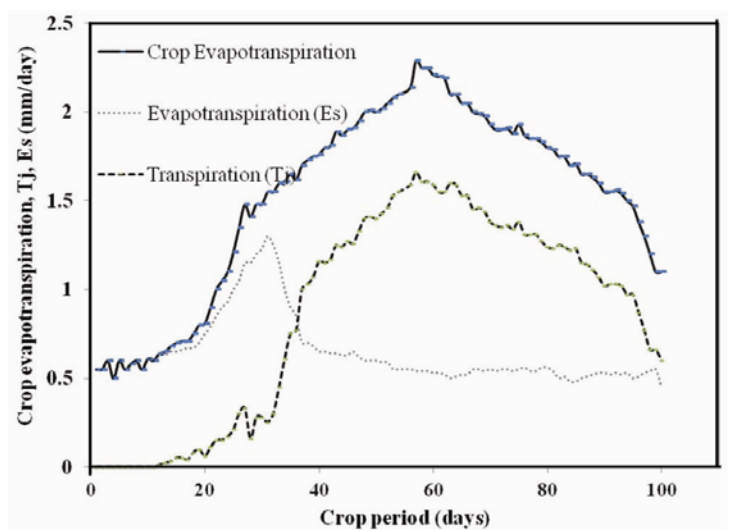


**Figure 4.** Daily crop evapotranspiration, transpiration and evaporation for pea.

**Results and discussion**

Ojha *et al.*<sup>22</sup> evaluated the Ojha and Rai<sup>33</sup> moisture extraction model for uniform root zone. Shankar *et al.*<sup>23</sup> developed a model for the nonlinear RWU parameter  $\beta$  of the Ojha and Rai<sup>33</sup> moisture extraction model.

$$\beta = 5.1128 T_s^2 - 6.117 T_s + 3.1545 \quad (15)$$

for  $0.07 \leq T_s \leq 0.98$

where  $T_s$  is given as<sup>23</sup>

$$T_s = \frac{T_{Jmax}}{Z_{Jmax}} \times t_{Peak} \quad (16)$$

Here  $T_{Jmax}$  is the maximum transpiration rate,  $Z_{Jmax}$ , maximum root depth and  $t_{Peak}$ , their time of occurrence during the crop period. In the present study  $\beta$  was obtained as 2.37 using maximum transpiration ( $T_{Jmax}$ ) 1.66 mm/day occurring 57 DAS and maximum root depth of 0.65 m.

The simulated soil moisture depletion in crop root zone was determined for some typical intervals during the crop period. The intervals selected for this purpose correspond to the duration between two rainfall events, two rainfall and irrigation event or two irrigation events. In pea crop typical periods were chosen as: 8–18 DAS (1–11 December), 28–38 (21–31 December) and 46–75 DAS (8–19 January). From Figure 5, it can be observed that simulated moisture depletion patterns are in close agreement with the observed moisture depletion. Error statisti-

cal parameters computed for comparing the simulated and observed moisture depletion patterns for different periods have been found in the following range: COD: 0.86 to 0.94, ARE: -2.14 to 4.5 and COV: 0.23 to 0.31. Details of error statistics for pea crop are given in Table 3.

It is evident from Figure 5 that the differences between the simulated and observed moisture depletion values in the middle layers are less compared to the top and the bottom layers. The model underestimates the soil moisture depletion in the top layers and overestimates moisture depletion in bottom layers. This may be because root density is maximum in the top layers, whereas it is minimum in the bottom layers of the root zone. As moisture uptake is a function of root density, moisture prediction can be improved in these layers if a root density function is considered in the root uptake model.

Varying soil moisture profiles in crop root zone represent the comparison between model-simulated and field-observed moisture values. For this purpose, few days in the crop period were chosen randomly. In case of pea crop, the pattern of moisture depletion at different depths on particular days shows similar patterns between observed and model-predicted values, which confirms the qualitative agreement between the two. Figure 6 shows the pattern of moisture depletion at different depths on particular days. The error statistics has been found to be within the following range; COD 0.72 to 0.95, ARE -3.2% to 11.1% and COV 0.06 to 0.19. The values of COD, ARE and COV for some typical days are: 15 DAS - 0.92, 2.3, 0.11; 55 DAS - 0.879, -1.4, 0.12 and 84 DAS - 0.86, 4.01, 0.17. It can be observed from Figure 6 that the simulated soil moisture profiles are in close agreement with the observed profiles on the days falling in between two rainfall/irrigation or rainfall and irrigation events. Better agreement between observed and simulated moisture depletion values during middle of the crop period is observed due to less uncertainty involved during the period. The days at the beginning or end of the duration (i.e. two rainfall, rainfall and irrigation and two irrigations events) are prone to high uncertainty and hence there may be poor agreement between observed and model-predicted values.

Soil moisture status at different root depths in the root zone gives an idea about the availability of moisture for plant moisture uptake. It is observed that in the upper part of the root zone where root density is high, moisture

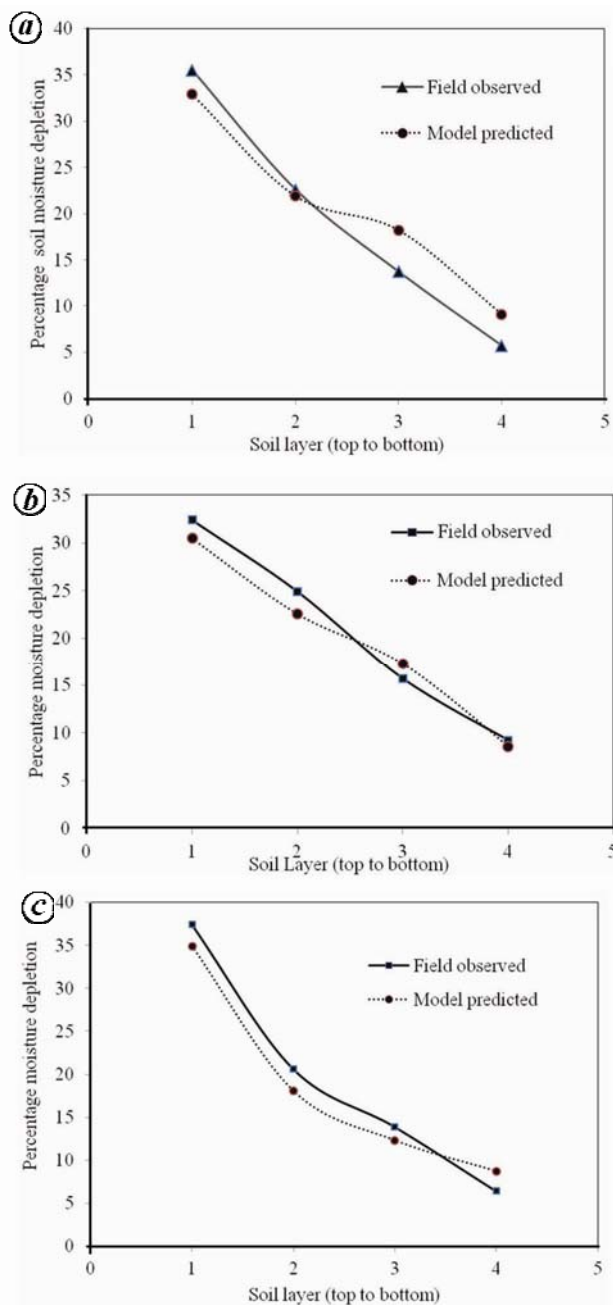


**Figure 5.** Model-predicted and field-observed soil moisture depletion for pea during the period 8–18 days after sowing (DAS) (a), 28–38 DAS (b), 46–57 DAS (c).

**Table 3.** Statistical errors of soil moisture depletion at different times of growth period

Crop	Period (days after sowing)	COD	ARE (%)	COV
Pea	8–18	0.94	-1.16	0.23
	28–38	0.89	-2.14	0.24
	46–57	0.86	4.5	0.31
	80–90	0.91	-1.2	0.20

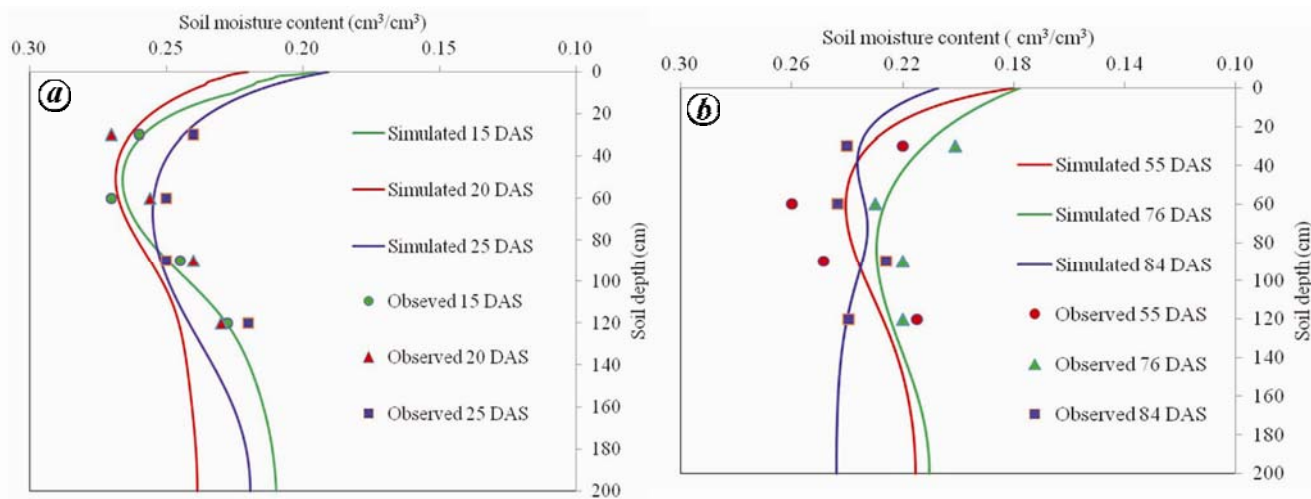


Figure 6. Model-predicted and field-observed soil moisture profiles for pea on 15, 20 and 25 DAS (a) and 55, 76 and 84 DAS (b).

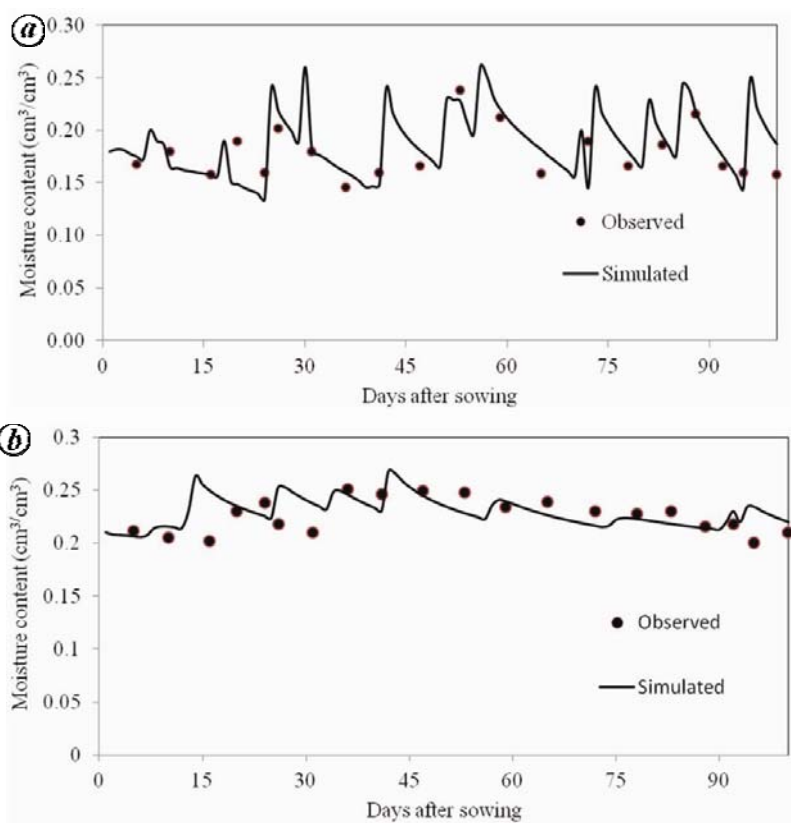


Figure 7. Model-predicted and field-observed soil moisture status for the entire crop period for pea at 30 cm depth (a) and 60 cm depth (b).

depletes very fast, whereas in the lower part of the root zone sufficient moisture for the plant moisture uptake is continuously available. Four typical depths have been selected (30, 60, 90 and 120 cm) for the study. Figure 7a and b shows the simulated and observed soil moisture status during crop period for pea at 30 and 60 cm root depth. It is evident from the figure that simulated soil moisture profile at particular depth throughout the crop

period is in close agreement with the observed soil moisture profile. The error statistics corresponding to the simulated and observed soil moisture content values on observation days spread throughout the crop period is given in Table 4.

From the perusal of error statistics it can be concluded that COD values corresponding to all the root zone depths are low, but there is good agreement between the simu-

**Table 4.** Error statistics for comparison of simulated and observed soil moisture status at different depths of root zone

Crop	Soil depth (cm)	ARE (%)	COV	COD
Pea	30	0.74	2.1	0.09
	60	0.77	5.5	0.12
	90	0.61	-3.12	0.08
	120	0.56	-4.15	0.13

lated and observed values. The significant small values of ARE and COV in all the cases strongly confirm the adequacy of simulated values. Over longer periods, field moisture predictions involve errors due to high variability in the unsaturated soil characteristics<sup>23,53</sup>. As the process in this case involves the whole crop period, a very high COD value is difficult to obtain, but low values of ARE and COV indicate that the deviation of simulated values from observed ones is within the range of acceptability. It is evident from the analysis of the simulated and observed soil moisture status that there is slightly larger deviation between simulated and observed moisture content in the upper and lower layers, compared to the middle layers. Close relationship of simulated and observed percentage moisture depletion values in the present study for pea indicates that the Ojha and Rai<sup>34</sup> root uptake model and the model for nonlinear uptake parameter  $\beta$  work well for sub-humid, sub-temperate agro-climatic zone for multilayer crop root zone<sup>24</sup>. Comparison of model-predicted and field-observed soil moisture depletion, soil moisture profiles and soil moisture status in the root zone of pea crop clearly demonstrates the nonlinear nature of root water uptake.

The agreement between the model-predicted and the observed moisture uptake indicators validates the suitability of the Ojha and Rai model for moisture extraction prediction. The important model input parameters, i.e. saturated moisture content ( $\theta_s$ ), constant  $n$ , field capacity and permanent wilting point, residual moisture content moisture ( $\theta_R$ ), the Ojha and Rai model parameters ' $\alpha$ ' and ' $\beta$ ' and saturated hydraulic conductivity ( $K_S$ ) have significant impact on the model output. Further studies on the role and effect of these parameters on moisture uptake prediction can bring in improvement in the model predictions.

## Conclusions

Modelling of root water uptake by plants is a difficult task, particularly in a country like India with diverse agro-climatic conditions. The present study was aimed at analysing the moisture prediction efficiency of a RWU model incorporating an empirical model for its nonlinear parameter. Good moisture prediction efficiency of the root uptake model which is validated from field experi-

ments signifies that the Ojha and Rai model can be utilized across different agro-climates. The following conclusions are drawn from this study:

1. A numerical model for predicting root water uptake in a multilayered/non-uniform crop root zone was developed and validated from field data. The model was based on a fully implicit finite difference scheme. Different boundary conditions at the top and bottom of the solution domain were provided, according to the field conditions.
2. The model-predicted soil moisture uptake indicators, i.e. moisture status at various depths, moisture depletion and soil moisture profile in the root zone are in agreement with experimental observations during the growth period of the crop.
3. The moisture flow in the unsaturated zone is highly nonlinear and involves large uncertainties. The modelled moisture uptake patterns show that precisely obtained field data are vital and important.

1. Kramer, P., The intake of water through dead root systems and its relation to the problem of absorption by transpiring plants. *Am. J. Bot.*, 1933, **20**, 481–492.
2. Burgess, S. S. O., Pate, J. S., Adams, M. A. and Dawson, T. E., Seasonal water acquisition and redistribution in the Australian woody phreatophyte, *Banksia prionotes*. *Ann. Bot.*, 2000, **85**, 215–224.
3. Ryel, R. J., Caldwell, M. M., Yoder, C. K., Or, D. and Leffler, A. J., Hydraulic redistribution in a stand of *artemisia tridentata*: evaluation of benefits to transpiration assessed with a simulation model. *Oecologia*, 2002, **130**, 173–184.
4. Brooks, J. R., Meinzer, F. C., Warren, J. M., Domec, J. C. and Coulombe, R., Hydraulic redistribution in a Douglas-fir forest: lessons from system manipulations. *Plant Cell Environ.*, 2006, **29**, 138–150.
5. Prieto, I., Mart, K., Mart, L., Manchego, S., Pugnaire, F. I. and Squeo, F. A., Hydraulic lift through transpiration suppression in shrubs from two arid ecosystems: patterns and control mechanisms. *Oecologia*, 2010, **163**, 855–865.
6. Luo, Y., Ou Yang, Z., Yuan, G., Tang, D. and Xie, X., Evaluation of macroscopic root water uptake models using lysimeter data. *Trans. ASAE*, 2003, **46**, 1–10.
7. Molz, F. J. and Remson, I., Application of an extraction term model to the study of moisture flow to plant roots. *Agron. J.*, 1971, **63**, 72–77.
8. Gardner, W. R., Dynamic aspects of water availability to plants. *J. Soil Sci.*, 1960, **89**, 63–73.
9. Molz, F. J., Remson, I., Fungaroli, A. A. and Drake, R. L., Soil moisture availability for transpiration. *Water Resour. Res.*, 1968, **4**, 1161–1169.
10. Hillel, D., van Beek, C. G. E. M. and Talpaz, H., A microscopic scale model of soil water uptake and salt movement to plant roots. *J. Soil Sci.*, 1975, **120**, 385–399.
11. Hainsworth, J. M. and Aylmore, L. A. G., Water extraction by single plant roots. *Soil Sci. Soc. Am. J.*, 1986, **50**, 841–848.
12. Nimah, M. N. and Hanks, R. J., Model for estimating soil water, plant and atmospheric interrelations. 1: Description and sensitivity. *Soil Sci. Soc. Am. Proc.*, 1973, **37**, 522–527.
13. Feddes, R. A., Kotwalik, P. J. and Zaradny, H., *Simulation of Field Water Use and Crop Yield*, Centre for Agricultural Publishing and Documentation, Wageningen, The Netherlands, 1978.

## RESEARCH ARTICLES

---

14. Afshar, A. and Marino, M. A., Model for simulating soil water content considering evaporation. *J. Hydrol.*, 1978, **37**, 309–322.
15. Molz, F. J., Models of water transport in soil plant system: a review. *Water Resour. Res.*, 1981, **317**, 1245–1260.
16. Marino, M. A. and Tracy, J. C., Flow of water through root soil environment. *J. Irrig. Drain. Eng. (ASCE)*, 1988, **114**, 558–604.
17. Li, K. Y., Boisvert, J. B. and Jong, R. D., An exponential root water uptake model. *Can. J. Soil Sci.*, 1999, **79**, 333–343.
18. Wu, J., Zhang, R. and Gui, S., Modeling soil water movement with water uptake by roots. *J. Plant Soil*, 1999, **215**, 7–17.
19. Vrugt, J. A., Hopmans, J. W. and Simunek, J., Calibration of a two dimensional root water uptake model. *Soil Sci. Soc. Am. J.*, 2001, **65**, 1027–1037.
20. Yadav, B. K. and Mathur, S., Modeling soil water extraction by plants using non-linear dynamic root density distribution function. *J. Irrig. Drain. Eng. (ASCE)*, 2008, **134**, 430–436.
21. Yadav, B. K., Mathur, S. and Siebel, M. A., Soil moisture dynamics modeling considering the root compensation mechanism for water uptake by plants. *J. Hydrol. Eng. (ASCE)*, 2009, **14**, 913–922.
22. Ojha, C. S. P., Hari Prasad, K. S., Shankar, V. and Madramootoo, C. A., Evaluation of a nonlinear root water uptake model. *J. Irrig. Drain. Eng. (ASCE)*, 2009, **135**, 303–312.
23. Shankar, V., Hari Prasad, K., Ojha, C. and Govindaraju, R. S., Model for nonlinear root water uptake parameter. *J. Irrig. Drain. Eng. (ASCE)*, 2012, **138**, 905–917.
24. Blizzard, W. E., Comparative resistance of the soil and the plant to water transport. *Plant Physiol.*, 1980, **66**, 809–814.
25. Amenu, G. G. and Kumar, P., A model for hydraulic redistribution incorporating coupled soil-root moisture transport. *Hydrol. Earth Syst. Sci.*, 2008, **12**, 55–74.
26. Burgess, S. S. O., Adams, M. A., Turner, N. C. and Ong, C. K., The redistribution of soil water by tree root systems. *Oecologia*, 1998, **115**, 306–311.
27. Schulze, E. D. *et al.*, Downward flux of water through roots (i.e., inverse hydraulic lift) in dry Kalahari sand. *Oecologia*, 1998, **115**, 460–462.
28. Smith, D. M., Jackson, N. A., Roberts, J. M. and Ong, C. K., Reverse flow of sap in tree roots and downward siphoning of water by *Grevillea robusta*. *Funct. Ecol.*, 1999, **13**, 256–264.
29. Hultine, K. R., Cable, W. L., Burgess, S. S. O. and Williams, D. G., Hydraulic redistribution by deep roots of a Chihuahuan Desert phreatophyte. *Tree Physiol.*, 2003, **23**, 353–360.
30. Ishikawa, C. M. and Bledsoe, C. S., Seasonal and diurnal patterns of soil water potential in the rhizosphere of blue oaks: evidence for hydraulic lift. *Oecologia*, 2000, **125**, 459–465.
31. Ludwig, F., Dawson, T. E., Kroon, H., Berendse, F. and Prins, H. H. T., Hydraulic lift in *Acacia tortilis* trees on an east African savanna. *Oecologia*, 2003, **134**, 293–300.
32. Brooks, J. R., Meinzer, F. C. and Gregg, J., Hydraulic redistribution of soil water during summer drought in two contrasting Pacific northwest coniferous forest. *Tree Physiol.*, 2002, **22**, 1107–1117.
33. Ojha, C. S. P. and Rai, A. K., Nonlinear root water uptake model. *J. Irrig. Drain. Eng. (ASCE)*, 1996, **122**, 198–202.
34. Richards, L. A., Capillary conduction of liquids through porous medium. *Physics (NY)*, 1931, **1**, 318–333.
35. Prasad, R., Influence of time step in the simulation modelling of evapotranspiration. *Sadhana: Proc. Indian Acad. Sci.*, 1984, **7**, 91–118.
36. Prasad, R., A linear root water uptake model. *J. Hydrol.*, 1988, **99**, 297–306.
37. Kang, S., Zhang, F. and Zhang, J., A simulation model of water dynamics in winter wheat field and its application in a semiarid region. *Agric. Water Manage.*, 2001, **49**, 115–129.
38. Yadav, B. K., Mathur, S. and Siebel, M. A., Soil moisture flow modeling with water uptake by plants (wheat) under varying soil and moisture conditions. *J. Irrig. Drain. Eng. (ASCE)*, 2009, **135**, 375–381.
39. Quijano, J. C., Kumar, P., Drewry, D. T., Goldstein, A. and Mission, L., Competitive and mutualistic dependencies in multispecies vegetation dynamics enabled by hydraulic redistribution. *Water Resour. Res.*, 2012, **48**, W05518.
40. Celia, M. A., Bouloutas, E. T. and Zarba, R. L., A general mass conservative numerical solution for the unsaturated flow equation. *Water Resour. Res.*, 1990, **26**, 1483–1496.
41. Van Genuchten, M. T., A closed form equation for predicting the hydraulic conductivity of unsaturated soil. *Soil Sci. Soc. Am. J.*, 1980, **44**, 892–898.
42. Remson, I., Hornberger, G. M. and Molz, F. J., In *Numerical Methods in Subsurface Hydrology*, Wiley, New York, 1971, pp. 165–182.
43. Ambrose Jr, R. B. and Roesch, S. E., Dynamic estuary model performance. *J. Environ. Eng. Div.*, 1982, **108**, 51–57.
44. Mendenhall, W. and Sincich, T., *Statistics for Engineering and Computer Sciences*, Dellen Publishing Co, San Francisco, 1988.
45. Gold, H. J., In *Mathematical Modelling of Biological Systems*, Wiley, New York, 1977.
46. Trout, T. J., Garcia-Castillas, I. G. and Hart, W. E., *Soil Water Engineering: Field and Laboratory Manual*, Academic Publishers, Jaipur, 1982.
47. Carsel, R. F. and Parrish, R. S., Developing joint probability distributions of soil water retention characteristics. *Water Resour. Res.*, 1988, **24**, 755–759.
48. Doorenbos, J. and Pruitt, W. O., Guidelines for predicting crop water requirement: FAO Irrigation and Drainage Paper No. 24, FAO, Rome, Italy, 1977, p. 156.
49. Allen, S. J., Measurement and estimation of evaporation from soil under sparse barley crops in northern Syria. *J. Agric. For. Meteorol.*, 1990, **49**, 291–309.
50. Campbell, G. S. and Norman, J. M., *An Introduction to Environmental Biophysics*, Springer Verlag, New York, 1998, 2nd edn.
51. Zhang, Y., Yu, Q., Liu, C., Jiang, J. and Zhang, X., Estimation of winter wheat evapotranspiration under water stress with two semi-empirical approaches. *Agron. J.*, 2004, **96**, 159–168.
52. Raes, D., Van Aelst, P. and Wyseure, G., ETref, ETcrop, ETsplit and deficit, a computer package for calculating crop water requirements. Reference manual, 1986.
53. Thomas, H. R. and Rees, S. W., A comparison of field monitored and numerically predicted moisture movement in unsaturated soil. *Int. J. Numer. Anal. Met. Geomech.*, 1991, **15**, 417–431.

**ACKNOWLEDGEMENTS.** We thank the Department of Civil Engineering, National Institute of Technology, Hamirpur and Department of Soil Science and Water Management, Dr Y.S. Parmar University of Horticulture and Forestry, Solan for providing all facilities during this study.

Received 21 January 2013; revised accepted 2 July 2013